Density Functional and Complete Active Space Self-Consistent Field Investigations on the Structure and Electronic Properties of TiC_x ($x = 2-4$) Clusters

R. Sumathi* and M. Hendrickx

Department of Chemistry, University of Leuven, Celestijnenlaan 200F, B-3001 Leuven, Belgium

Received: January 8, 1998; In Final Form: March 20, 1998

The structures and energies of the previously not studied titanium carbide TiC_x ($x = 3-4$) clusters have been investigated by density functional theory (DFT) using the hybrid B3LYP functional in their singlet, triplet, and quintet potential energy surfaces. The planar four-membered ring structure **VIs**, otherwise called the "fan" structure, with a transannular Ti−C bond is the global TiC_3 minimum and 21.5 kcal/mol more stable than the transannular C−C bond structure, **VIIt** ("kite" structure) at the DFT level. Both cyclic structures are energetically favored over a linear quintet minimum. Electronic structure and the nature of bonding in the various electronic states of the fan and kite structures of TiC_3 have been well-characterized at the complete active space self-consistent field (CAS(12,12)) level. For the TiC_4 cluster, two nonplanar structures have been considered in addition to three linear, fan, and kite geometries. Nonplanar structures are characterized as higher energy minima. The harmonic frequencies calculated using the DFT method for the Ti−C stretching vibrations in TiC_x are in good agreement with the recent experimental results supporting the identification of new tetra- and pentaatomic titanium−carbon clusters.

Introduction

Castleman and co-workers,[1] in the beginning of this decade, produced Ti_nC_m clusters (met-cars) in molecular beams by reacting transition metal vapors with a variety of hydrocarbons. Since then, a number of investigations[2] have been carried out on Ti_8C_{12} and related species with a view to understand the electronic bonding in met-cars and the relative stabilities of the met-cars and cubic structures. Despite the intensive research on met-cars, all these years since its discovery, the structure and bonding of these unique clusters are still not well-understood. However, a systematic and clear understanding of the detailed structure and bonding of the small metal−carbide clusters would lead to valuable insights into the growth and formation of the met-cars.[3−7] In this regard, the very recent photoelectron spectral studies by Wang et al.[8] provide the first and only spectroscopic and electronic information on TiC_x ($x = 2-5$) clusters. In the absence of any other theoretical or experimental investigations on these systems, these authors interpreted their results on the ground-state vibrational frequencies as well as the adiabatic electron affinities of TiC_x by using ring-type structures that are known to be the ground-state structure for similar YC_x[9] and LaC_x[10−13] clusters.

Our interest in met-cars is to identify the building blocks of M_8C_{12} and to investigate the clustering phenomenon. In this regard, we wish to characterize the simpler Ti−C compounds, the potential candidates for the building blocks, namely, TiC, TiC_2, TiC_3, Ti_2C, Ti_2C_2, and Ti_2C_3, by using ab initio calculations. The simplest compound, TiC, has already been studied at CASSCF,[14,15] MRCI,[14,15] and DFT[15] levels. All calculations confirm that the ground state of TiC is the $^3\Sigma^+$ state with the equilibrium Ti−C distance varying from 1.66 Å to 1.76 Å with different levels of calculation. The next homologue, titanium dicarbide, has been investigated by us[16] at the hybrid density functional (B3LYP), internally contracted multireference configuration interaction (MRCI), and complete active space self-consistent field (CASSCF) levels. The geometry of TiC_2 is found to be a triangular C_{2v} structure with a 2-fold coordination of a C_2 moiety to Ti. Also, almost 10 electronically excited states are calculated to be separated by less than 40 kcal/mol from the ground state. Our theoretical prediction is in very good agreement with the recent experimental observation of rich low-lying electronic excited states by Wang et al.[8] The B3LYP computed harmonic vibrational frequency for the symmetric Ti−C stretching vibration in TiC_2 is 587 cm^{-1}, which is quite close to the experimental absorption[8] at 560 cm^{-1}.

To our knowledge, there exists no theoretical study on TiC_x ($x > 2$) systems. Hence, the present study continues the series of carbon−titanium clusters, concentrating on a detailed ab initio theoretical analyses of the potential energy surfaces of TiC_3 and TiC_4 in their different electronic states. The results will be compared with the experimentally and theoretically well-studied lanthanum metal carbides. Besides being interesting from the point of view of met-cars, the electronic structure of titanium and the compounds it forms are intriguing, since it is the simplest group IVB analogue of the well-studied group IVA elements, C and Si. Within the group IVA elements, differences exist in the bonding and structure of carbon clusters as compared to silicon clusters. The isoelectronic (valence electrons) C_4 favors a linear structure[17,18] over the rhombic form, while Si_4 prefers a rhombic form.[19,20] In silicon-containing carbon clusters, the photoelectron spectra[21] of SiC_3^- suggests it to be linear. However, according to the results of the calculation[22] for the neutral SiC_3, the rhomboidal ring structure is 4.1 kcal/mol more stable than the linear triplet Si−C−C−C isomer. Hence, it is worthwhile to see the impact of the fundamental differences between s^2p^2 and s^2d^2 configurations. We present here the structure and energetics of the various possible conformations of TiC_3 and TiC_4 in their singlet, triplet, and quintet multiplicities. We consider for DFT optimization various possible nuclear

S1089-5639(98)00733-6 CCC: $15.00
Published on Web 05/29/1998

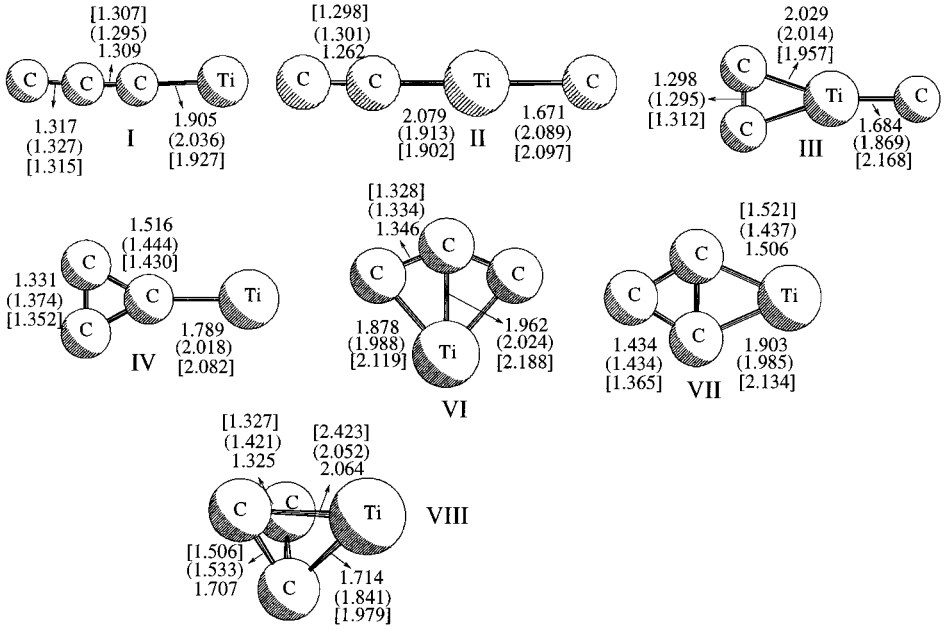

Figure 1. Optimized geometries for the singlet, triplet, and quintet isomers of TiC_3 at the B3LYP level of theory, with triplet and quintet geometries, respectively, in parentheses and square parentheses. Bond lengths are given in Å.

arrangements, and we then investigate the electronic structure for the most stable minima by using the multiconfiguration approach.

Computational Details

The calculations presented here were performed by using the density functional theory. The exchange functional in the hybrid B3LYP[23] method is comprised of three terms, including the Hartree−Fock exchange functional. The correlation functional is that of Lee, Yang, and Parr.[24] To characterize the nature of the stationary points, harmonic vibrational frequencies have also been calculated at the DFT level. The titanium basis set was a (14s,11p,6d,3f/8s,6p,4d,1f) formed from Wachter's[25] (14s,9p,-5d) basis set with the addition of Hay's diffuse[26] 3d function. The f Slater type function (STF) exponent was taken from Bauschlicher et al.,[27] and the Gaussian type function (GTF) exponents were derived by using Stewart's contraction fits.[28] For carbon, the standard DZP (9s,5p,1d/4s,2p,1d) basis set was used. B3LYP calculations were carried out with MULLIKEN[29] program. The favored geometries at the B3LYP level for TiC_3 have then been characterized at the multiconfiguration level to understand the nature of bonding and the electronic structure of TiC_3. The CASSCF optimizations included 12 out of 16 valence electrons. The four valence electrons corresponding to the C−C σ bonds have been kept inactive. The 12 active orbitals included the lone pairs ($9a_1$ and $4b_2$), π ($3b_1$ and $10A_1$), π^* orbitals of C_3, Ti−C σ bond ($5b_2$), and the metal d orbitals. The calculations were carried out by choosing the *z*-axis and the *yz*-plane as the C_2-axis and the molecular plane, respectively. MOLPRO-96[30] has been employed for CAS(12,12) optimizations.

Results and Discussion

The ground state of titanium carbides are formed from the ground $3d^24s^2$ (^{3}F) state of titanium and one of the low-lying singlet or triplet states of the C_n clusters. The lowest excited state of titanium, $3d^34s^1$ (^{5}F), is only 0.8 eV above its ground

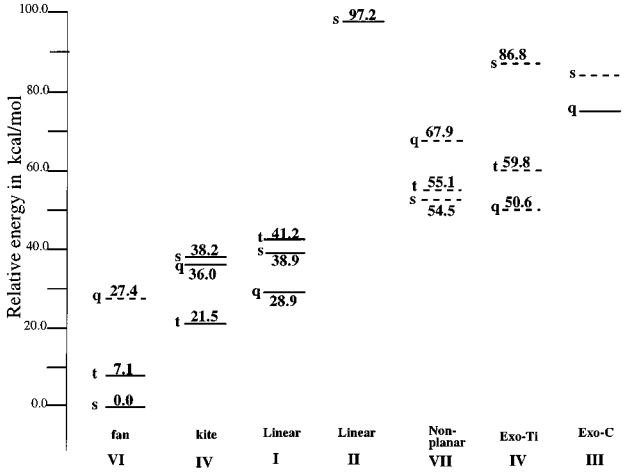

Figure 2. Plot of the relative energies (kcal/mol) of the various isomers in different electronic states of the TiC_3 cluster.

state,[31] and this state is responsible for the bonding[14] in TiN, TiO, and TiC. Therefore, it is likely that this state plays a significant role in the bonding in TiC_n too. Hence, except for the possible septet electronic states, the geometry search has been carried out for singlet, triplet, and quintet multiplicities. Geometry optimizations have been performed for the various electronic states at the B3LYP level, starting from different nuclear arrangements that included linear (I, II), planar three-membered cyclic (III, IV, V), planar four-membered cyclic (V, VI), and the nonplanar tetrahedral (VII) geometries. The B3LYP optimized geometries of all investigated structures for TiC_3 and TiC_4 in their singlet, triplet, and quintet states are displayed in Figures 1 and 4, respectively. The numbers in parentheses and square parentheses correspond to the optimized values on the singlet and quintet surfaces, respectively. The relative energy of all the structures in various electronic states of TiC_3 is shown in Figure 2, while that of TiC_4 is shown in Figure 5. The vibrational frequencies of TiC_3 and TiC_4 are tabulated, respectively, in Tables 1 and 2, however, only for the minimum energy structures. The CAS(12,12) optimized structures of the various excited states of the "fan" and "kite"

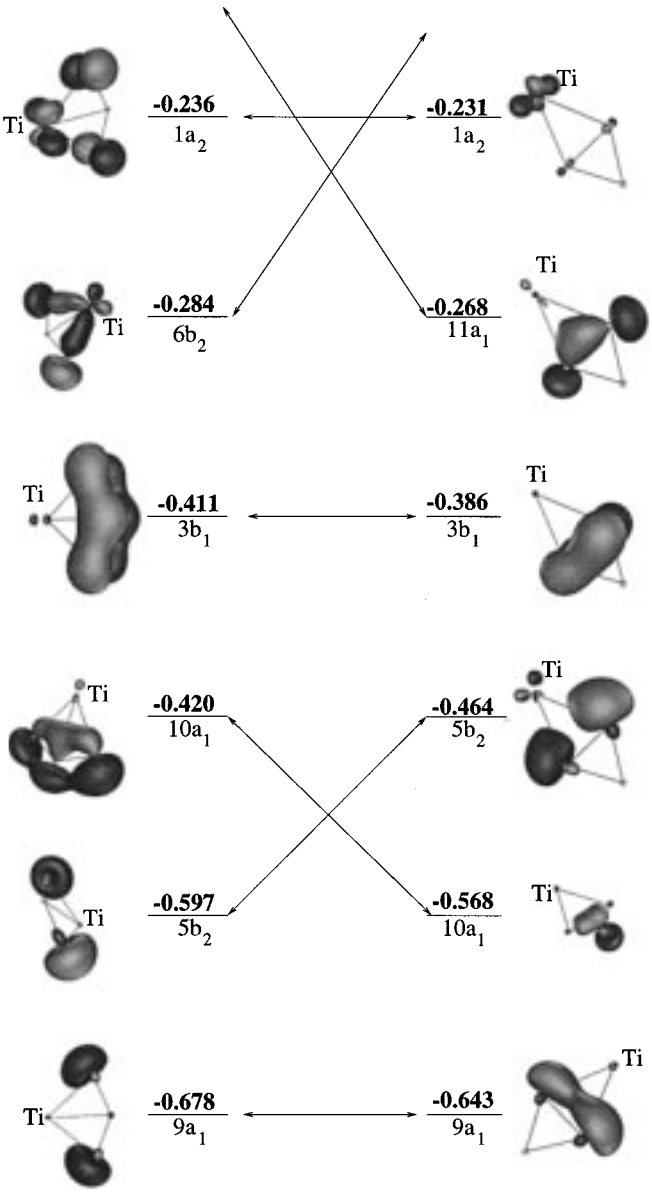

Figure 3. CAS(12,12) orbital correlation diagram for bond-stretch isomerism in TiC_3.

TABLE 1: Unscaled B3LYP Harmonic Vibrational Frequencies of the Various Minima on the Singlet, Triplet, and Quintet Potential Energy Surfaces of the TiC_3 Molecule

species	frequecies in cm^{-1}	exptl[a]
Is	171.8, 206.0, 413.9, 458.5, 1408.9, 2017.2	
Iq	134.4, 349.4, 368.8, 448.4, 1273.7, 1923.1	
IIs	106.9, 158.5, 210.4, 395.1, 860.8, 1806.9	
IIIq	30.7, 95.8, 423.3, 548.5, 660.4, 1804.7	
VIs	**465.3**, 591.2, **686.5**, 833.6, 1281.3, 1531.4	**650**
VIt	402.9, 408.2, 591.0, 765.5, 1268.8, 1547.8	
VIIs	215.7, 490.4, 518.6, 694.3, 981.9, 1342.4	
VIIt	312.3, 459.5, 544.5, 864.6, 1090.1, 1417.4	
VIIq	287.4, 337.7, 388.9, 861.6, 1119.9, 1599.7	

[a] Reference 8 in the text.

isomers of TiC_3 are given in Table 3 along with their electronic configuration.

TiC_3. *Linear Structures*. The linear isomer of main interest contains a terminal titanium atom showing the preference of titanium not to partake in multiple bonding. The quintet form **Iq** ($C_{\infty v}$) is the most favored electronic configuration over the triplet or singlet states via Hund's rule and displays strong C−C and Ti−C bonding as expected for a cumulene-like valence structure and is a minimum on the B3LYP potential energy surface, PES. Its calculated C−C bond lengths of ∼1.32 Å are intermediate between that of a normal C−C double bond length in ethylene (1.35 Å) and a normal triple bond in acetylene (1.21 Å). The C−Ti bond length of 1.93 Å is typical of a Ti═C double bond. The geometry of the triplet structure **It** differs much from that of the quintet with respect to the C−Ti bond length (0.11 Å). Even though the rhombic structure **VI** is the preferred geometry on the singlet and triplet surfaces, the linear isomer **I** is a stable minimum and is a highly competitive isomer on the quintet surface.

The linear isomer with an internal Ti atom **IIq** lies 68 kcal/mol above **Iq**. The increase in energy could probably be due to the increased Ti−C pi bonds at the expense of C−C π bonds. The Ti−C bond distances show significant differences (∼0.2 Å). The isomer **IIt** can be visualized as the addition of atomic carbon with the linear Ti−C−C structure. However, the C−Ti−C bond distances in the singlet surface suggest it to be the addition of Ti−C to C_2 moiety, and this structure is a local higher energy minimum only on the singlet surface.

Three-Membered Ring Structures. Three possible three-membered ring structures, viz., **III**, **IV**, and **V**, have been considered for geometry optimization. The viable three-membered ring and also a minimum on the PES is the isomer **IIIq**, which contains an exocyclic carbon attached to Ti of the TiC_2 ring. However, this isomer lies approximately 76 kcal/mol above the most stable conformer of TiC_3 (**VIs**). An analogous isomer for LaC_3[13] has not been considered, while such an isomer has been characterized as a higher energy minimum in the case of SiC_3.[22] In terms of the energetic behavior, the most favorable three-membered ring structure is **IV** with the titanium atom exocyclic to the ring. However, the vibrational analysis shows this structure as a transition state with a single imaginary frequency, 222i cm^{-1}. Analysis of the eigenvectors corresponding to the negative eigenvalue of the force constant matrix suggests it to be the transition state for the degenerate rearrangement to the "fan" isomer, **VI**. Geometric searches for the conformer **V** with an exocylic carbon attached to the carbon of a TiC_2 ring (not shown in Figure 1) led to the most favorable four-membered ring structure, **VI**. In summary, all three-membered ring structures except **IIIq** are either saddle points with respect to the degenerate rearrangement or stationary points of higher order. A similar behavior has been observed for the analogous three-membered ring[22] structures of SiC_3 and Si_2C_2 clusters.[20] However, a three-membered ring with an exocyclic lanthanum was reported[13] to be a higher energy minimum at DFT and MP2 levels.

Four-Membered Ring Structures. Two probable cyclic structures, viz., **VI** or the "fan" structure and **VII** or the "kite" structure, involving all four atoms of TiC_3 have been considered for optimization in their lowest singlet, triplet, and quintet states. Structure **VIs** with a transannular Ti−C bond is the most favorable structure. Structure **VI** has an inverted tricoordinate titanium as well as an inverted tricoordinate carbon atom. These inverted tricoordinate sp^2-hybridized carbon and X (B, Si, Be) atoms are well-documented[32] for rhombic C_3Be, C_3Si, C_3BH and C_2Si_2[20] systems. Both fan and kite structures in these molecules represent a set of bond-stretch isomers and have been shown[32] to be related via a level-crossing mechanism. However, in the case of C_3Be, C_3Si, and C_3BH, the isomer analogous to **VII** with a transannular C−C bond is predicted to be the most stable isomer.

The transannular Ti−C distance in the $^1A_1$ state of structure

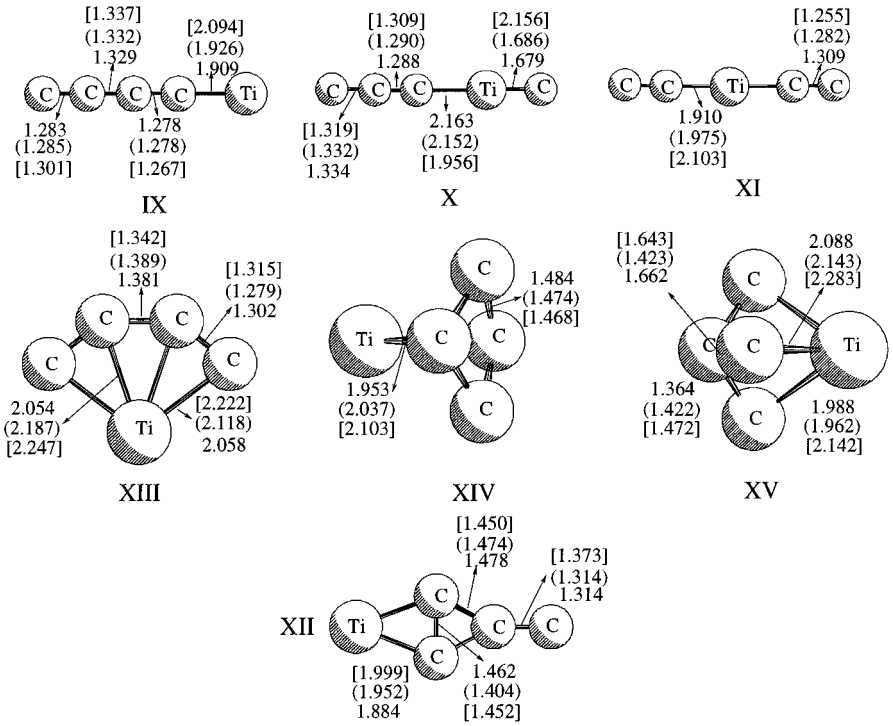

Figure 4. Optimized geometries for the singlet, triplet, and quintet isomers of TiC_4 at the B3LYP level of theory, with triplet and quintet geometries, respectively, in parentheses and square parentheses. Bond lengths are given in Å.

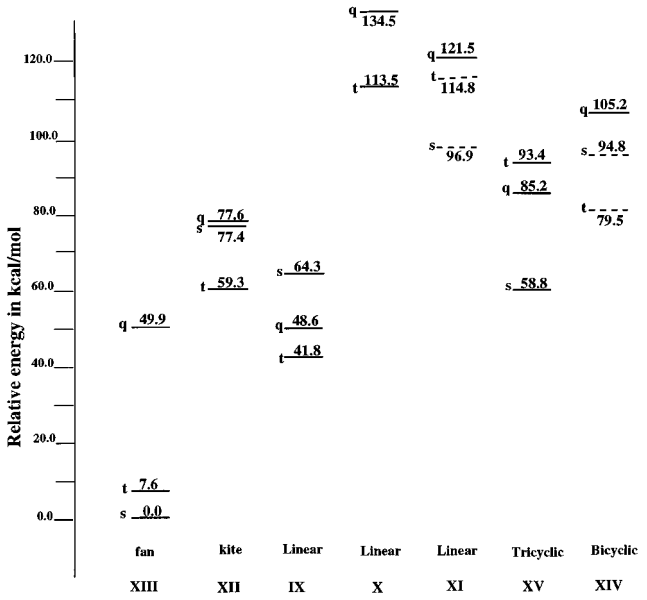

Figure 5. Plots of the relative energies (kcal/mol) of the various isomers in different electronic states of the TiC_4 cluster.

VI is 1.962 Å and is, therefore, indicative of significant Ti−C bonding across the ring. The B3LYP optimized value of CCC angle equals 132.3°. Triplet and quintet forms of **VI** show distinct differences with its singlet structure. Most importantly, the transannular Ti−C distance increases from singlet (1.962 Å) to triplet (2.024 Å) to quintet (2.188 Å) states. Also, the peripheral Ti−C distances increase in the same way, and as a consequence the C−C distances decrease. The C−C bond lengths in **VI** vary from 1.35 Å, to 1.33 Å, while varying the multiplicity of the state, and this magnitude corresponds to a carbon−carbon double bond. The structure is significantly different from the correponding SiC_3 isomer.[22] In the latter, the transannular Si−C distance is shorter than the peripheral Si−C distances. Hence, its bonding was explained as the complexation of Si to the middle carbon of the linear C_3. In the rhombic form of TiC_3, the peripheral Ti−C bonds are much stronger (Mulliken bond order = 1.83) compared to the transannular Ti−C bonds (Mulliken bond order = 0.68). The harmonic vibrational frequencies of **VIs** are tabulated in Table 1. As can be seen, the symmetric and asymmetric C−C stretching vibrations occur at 1281 (a_1) and 1531 (b_1) cm^{-1}, respectively. The Ti−C stretching frequencies are symmetrically coupled and the asymmetric and symmetric stretches occur, respectively, at 465 (b_1) and 686 (a_1) wavenumbers. In TiC_2, the symmetric Ti−C stretching vibration was calculated to absorb at 587 cm^{-1} at the same level of calculation. It is appropriate to mention that these computed values are in good agreement with the experimentally observed vibrational frequencies of TiC_2 (560 cm^{-1}) and TiC_3 (650 cm^{-1}).

Structure **VII** also corresponds to a four-membered ring, however, involving a transannular C−C distance of 1.44 Å, and, hence, is indicative of significant across-the-ring C−C bonding. The transannular C−C distance increases from triplet (1.436 Å) to singlet (1.506 Å) to quintet (1.521 Å). In **VIIt**, the Mulliken bond orders for the C−C and Ti−C bonds are 1.35 and 1.14, respectively. It involves two π bonding electrons delocalized on the C_3 ring. The corresponding **VIIs** singlet has these π electrons delocalized over the whole TiC_3 ring, and hence the Ti−C distance in the singlet (1.90 Å) is shorter than that in the triplet and has a partial multiple bond (Mulliken bond order = 1.49). However, isomer **VII** is around 21.5 kcal/mol higher in energy compared to the transannular Ti−C ring. The vibrational analysis of **VII** shows it to be a minimum on the singlet, triplet, and quintet potential energy surfaces.

In addition to these planar four-membered ring structures, we also have investigated a nonplanar structure **VIII**. Though such a nonplanar structure has not been obtained for the isomers of SiC_3 and Si_2C_2, we found it to correspond to a minimum[33] in the case of Ti_2C_2. However, our calculations on the nonplanar structure for TiC_3 reveal it to be a saddle point on all three electronic surfaces. Structure **VIII** can be visualized as the

TABLE 2: Unscaled B3LYP Harmonic Vibrational Frequencies of the Various Minima on the Singlet, Triplet, and Quintet Potential Energy Surfaces of the TiC_4 Molecule

species	frequecies in cm^{-1}	exptl[a]
IXs	115.2, 216.7, 239.3, 419.7, 523.7, 527.9, 1015.0, 1875.6, 2138.9	
IXt	106.6, 179.1, 240.9, 401.3, 479.0, 534.2, 1105.6, 1878.9, 2093.6	
IXq	96.6, 222.9, 237.3, 326.2, 407.4, 502.4, 962.8, 1801.8, 2044.6	
Xt	94.2, 106.2, 145.9, 301.4, 334.4, 425.7, 807.4, 1286.3, 1932.9	
Xq	44.1, 66.5, 180.6, 413.4, 419.2, 441.0, 573.4, 1431.9, 1909.9	
XIq	32.23, 163.5, 169.0, 258.5, 265.5, 357.2, 452.2, 1869.2, 1885.0	
XIIs	118.7, 165.2, 432.0, 446.9, 514.1, 875.3, 982.3, 1111.9, 1740.6	
XIIq	134.6, 221.8, 392.9, 405.2, 474.1, 870.9, 908.2, 1123.9, 1528.1	
XIIIs	256.1, 423.9, 449.8, 516.4, 594.7, 600.6, 1061.9, 1638.7, 1771.5	
XIIIt	251.9, 391.1, 399.6, **472.2**, 473.6, 601.1, 1055.5, 1789.2, 1882.7	440
XIIIq	156.9, 353.8, 356.5, 450.6, 458.5, 483.9, 1056.1, 1531.5, 1801.7	
XIVq	256.1, 311.1, 421.8, 431.8, 663.0, 780.4, 819.6, 851.2, 1215.6	
XVs	132.5, 241.9, 448.0, 522.9, 608.3, 737.1, 797.9, 1237.9, 1470.4	
XVt	181.9, 193.1, 442.5, 455.1, 572.7, 691.4, 1162.0, 1163.3, 1206.3	
XVq	187.5, 404.2, 430.2, 515.0, 585.4, 637.2, 738.8, 1174.6, 1205.2	

[a] Reference 8 in the text.

TABLE 3: Summary of CASSCF Calculations on (a) Fan and (b) Kite Isomers of TiC_3[a]

isomer	state	coefficient	occupation	R(Ti−C)	R(C−C)	trans(X−C)	ΔE
(a)	$^1A_1$	−0.89	$10a_1^2 3b_1^2 6b_2^2 1a_2^2$	1.959	1.349	2.013	0.0
(a)	$^3B_2$	0.90	$10a_1^2 4b_1^1 6b_2^2 1a_2^1$	2.110	1.338	2.111	21.5
(a)	$^3A_2$	−0.77	$10a_1^2 4b_1^1 6b_2^1 1a_2^2$	2.132	1.352	2.185	22.3
(a)	$^3A_2$	−0.90	$11a_1^1 3b_1^2 6b_2^2 1a_2^1$	2.058	1.332	2.084	24.1
(a)	$^1A_2$	0.64	$11a_1^1(\alpha) 3b_1^2 6b_2^2 1a_2^1(\beta)$	2.049	1.334	2.082	30.2
		−0.64	$11a_1^1(\beta) 3b_1^2 6b_2^2 1a_2^1(\alpha)$				
(a)	$^3B_2$	0.84	$11a_1^1 3b_1^2 6b_2^1 1a_2^2$	2.078	1.334	2.133	33.5
(a)	$^3A_1$	0.87	$10A_1^2 3b_1^2 6b_2^2 1a_2^1 2a_2^1$	2.145	1.345	2.109	38.1
(a)	$^1B_2$	−0.58	$11a_1^1(\alpha) 3b_1^2 6b_2^1(\beta) 1a_2^2$	2.092	1.332	2.178	38.6
(a)	$^3B_1$	−0.87	$11a_1^1 4b_1^1 6b_2^2$	2.339	1.315	2.286	41.4
(a)	$^1A_1$	−0.91	$11a_1^2 3b_1^2 6b_2^2$	2.241	1.301	2.168	46.5
(b)	$^3A_2$	0.73	$12a_1^1 3b_1^2 5b_2^2 1a_2^1$	2.263	1.362	1.557	23.0
(b)	$^3B_1$	−0.65	$12a_1^1 4b_1^1 5b_2^2$	2.303	1.358	1.543	23.1
(b)	$^3B_2$	−0.96	$11a_1^2 4b_1^1 5b_2^2 1a_2^1$	2.044	1.444	1.456	23.8
(b)	$^1B_1$	0.47	$12a_1^1(\alpha) 4b_1^1(\beta) 5b_2^2$	2.289	1.358	1.532	35.9
(b)	$^1A_1$	0.89	$11a_1^2 3b_1^2 5b_2^2 1a_2^2$	1.937	1.439	1.603	45.1
(b)	$^3A_1$	0.94	$12a_1^1 13a_1^1 3b_1^2 5b_2^2$	2.037	1.429	1.409	47.7
(b)	$^1A_1$	0.78	$12a_1^2 3b_1^2 5b_2^2$	2.035	1.439	1.445	62.3

[a] Coefficients and geometries are taken from the CASSCF minimum. Bond lengths in Å, ΔE in kcal/mol.

cycloaddition product of C_2 to Ti−C molecule. We present here the structure for the sake of completeness.

Figure 2 presents the relative energy of the various states of all the isomers investigated in the current study for TiC_3. The global minimum on the TiC_3 potential energy surface corresponds to **VIs** and has other minima on the singlet (**VIIs**, **IIs**), triplet (**VIt**, **VIIt**, **It**), and quintet (**VIIq**, **Iq**, **IIIq**) surfaces. The solid lines correspond to minima, while the dotted lines represent saddle points and stationary points of higher order.

CAS(12,12) Characterization of Isomers VI and VII. For the fan structure of the TiC_3 molecule, the important valence orbitals participating in the bonding scheme are shown in Figure 3 along with those for the kite structure. The electronic configuration of the fan TiC_3 ($^1A_1$) structure is $10a_1^2 3b_1^2 6b_2^2 1a_2^2$, out of which the core orbitals correspond to a $7a_1^2 2b_1^2 3b_2^2$ scheme. The closed $8a_1$ and $4b_2$ orbitals correspond to C−C σ bonds and are not included in the CAS active space. The closed $9a_1$ and $5b_2$ orbitals are predominantly the lone pairs localized on the peripheral carbons and are directed toward the titanium atom. The π orbitals of the C_3 moiety transform as a_1 ($10a_1$) and b_1 ($3b_1$) irreducible representations under the symmetry operations of the C_{2v} point group. They involve two π bonding electrons delocalized completely over the C_3 unit, resulting in a strong peripheral C−C bonding. It is worthwhile to mention that the transannular Ti−C bond acquires some stability from the $10a_1$ orbital. While the closed $6b_2$ orbital corresponds to the three center−two electron (3c−2e) Ti−C σ bond involving the d_{yz} orbital of the metal, the doubly occupied $1a_2$ orbital hosts the π back-bonding between the metal d_{xy} orbital and the empty π orbital of the C_3 unit located on the terminal carbons. Thus, the $6b_2$ contributes to the σ donation from the C_2 fragment, and consequently the metal d_{yz} orbital exerts a strong σ antibonding interaction with the ligand orbitals and as a result is placed energetically well above the other d orbitals. We have optimized the structure of 12 different states of symmetry and multiplicity at the CAS(12,12) level. The lowest triplet state ($^3B_2$) is about 20 kcal/mol above the ground state and has the two unpaired electrons in d_{xy} ($1a_2$) and d_{xz} ($4b_1$) orbitals of the metal. A careful analysis of the energetics of the different excited states suggests the ordering of the metal orbitals in the fan structure of TiC_3 to be d_{xy} (π^*) < d_{xz} (π) < $d_{x^2-y^2} \approx d_{z^2} < d_{yz}$ (σ).

The electronic configuration of the kite TiC_3 ($^1A_1$) structure is $11a_1^2 3b_1^2 5b_2^2 1a_2^2$, with the same core framework as the fan structure. The closed $8a_1$ and $4b_2$ orbitals are the C−C sigma bonds. The closed $9a_1$ and $5b_2$ orbitals depict the lone pair character. The $3b_1$ orbital corresponds to the ligand π orbital. The doubly occupied $6b_2$ orbital of the fan structure is left vacant in the kite conformer. The other active orbital in the CAS space, viz., the $10a_1$ orbital, corresponds to the transannular C−C σ bond with appreciable lone pair character on the symmetry unique carbon atom. Thus, the three C−C σ bonds in the cyclic

C_3 unit can be identified with $8a_1$, $10a_1$, and $4b_2$ orbitals. The correlation diagram for TiC_3 (Figure 3) points out a crossing of the $11a_1$ orbital of the kite isomer and the $6b_2$ orbital of the fan isomer to unoccupied molecular orbitals, respectively. This simple level crossing mechanism explains the bond-stretch isomerism. In TiC_3, the fan isomer is more stable compared to the kite isomer, in contrast to XC_3 (X = BH, Be, Si) systems. This is essentially due to the strong Ti−C σ bonds formed with the d_{yz} orbital of the metal. The overlap is very effective with the d orbital of Ti compared to the p orbitals of X. The lobes of the d orbitals are appropriate for this bent 3c−2e bond. The $11a_1$ orbital of the kite isomer has its electron density smeared away from the C−C bond and toward the metal atom. Indeed, it reflects the degree of electron density depletion from the C−C bond toward the Ti atom. Consequently, it leads to strengthening of the peripheral C−Ti bonds. Hence, it is obvious in the kite structure with short cross-ring C−C distances that the heteroatoms "interact" with a side of the cyclic C_3 unit. The strength of this interaction varies with the electronic state, and it determines whether there remains cross-ring C−C bonding. The transannular C−C distance varies appreciably with the nature of the electronic state (see Table 3). The ground state of the kite isomer corresponds to a triplet state. It is worthwhile to mention that the DFT method could reproduce this state as the low-lying state. However, the DFT-predicted Ti−C bond lengths are relatively shorter and the C−C bond lengths are relatively longer than those of the CAS(12,12) optimized structures. Nevertheless, the energy difference between the ground states of the fan and kite isomers is 23.1 and 21.5 kcal/mol, respectively, at CAS(12,12) and B3LYP levels. Thus, the DFT-predicted value is in very good agreement with the CAS-(12,12) results.

TiC_4. Three linear isomers, a planar four-membered ring with an exocyclic carbon or the kite isomer (**XII**), a planar five-membered ring (**XIII**) or the fan isomer, and two tricyclic nonplanar (**XIV** and **XV**) nuclear arrangements have been considered (Figure 4) for geometry optimizations in various electronic states.

Linear Structures. Three possible linear structures, viz., a terminal titanium **IX**, with an internal titanium **X** and titanium in the middle **XI**, have been considered for optimization. As discussed under TiC_3, the isomer **IX** with a terminal titanium is energetically more favored over the other two linear isomers. The carbon atoms are multiply bonded in the linear chain. The C−Ti distance decreases from **IXq** to **IXt** to **IXs**, and this trend is in contrast to that observed in the case of TiC_3. In the latter, it increases from **Iq** to **It** to **Is**. Energetically, **IXt** is more stable among the linear isomers. Nevertheless, **IXt** lies 41.8 kcal/mol above the global minimum, **XIIIt**. The vibrational analysis characterizes it as a minimum on all three surfaces. The relative stability of the linear structure over the ring structure decreases along the series, TiC_2 (ΔE =14.5 kcal/mol) → TiC_3 (ΔE = 28.9 kcal/mol) → TiC_4 (ΔE = 41.8 kcal/mol).

An alternative linear isomer with an internal titanium **X** has been identified as a higher energy minima on its quintet and triplet surfaces. The C−Ti distances show appreciable differences in **Xt**, one being significantly smaller (1.686 Å) and the other significantly longer (2.153 Å) than the Ti−C double bonds. Isomer **Xt** could be visualized as the addition of TiC to C_3. The geometry of **Xq** is suggestive of a linear :Ti═C═C═C: molecule bonded to a ^{3}P carbon through the titanium lone pair. The highly symmetrical ($D_{\infty h}$) linear isomer **XI** is a minimum on its quintet surface and a higher order saddle point on its singlet and triplet surfaces. The quintet surface can well be represented as :C≡C−Ti−C≡C:. The bond orders calculated from the Mulliken population analysis for the C−C and Ti−C bonds are 2.66 and 0.90, respectively.

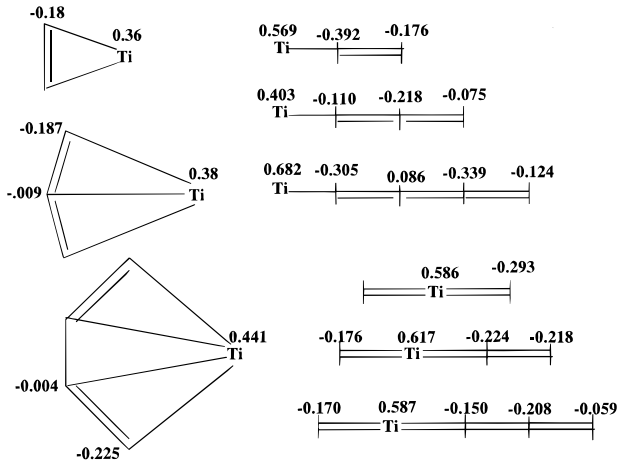

Figure 6. Atomic charges and dipole moments (in debye) for the different structures of TiC_x (x = 2−4).

Four- and Five-Membered Ring Structures. Isomer **XII** could be visualized as the kite isomer of TiC_3 with an external carbon. All carbons are multiply bonded. It is a higher energy minimum on TiC_4 potential energy surface, and it lies even higher than the linear structure **IX**. In the case of LaC_4 and SiC_4 too, the corresponding kite isomer is disposed far above (85.7 kcal/mol) the fan structure.

The global minimum is the fan structure **XIII** (see Figure 5) in its triplet multiplicity. The peripheral Ti−C bonds are shorter than the transannular Ti−C bonds as observed in TiC_3. The calculated bond orders using Mulliken population analysis for the peripheral and the transannular Ti−C bonds are, respectively, 0.99 and 0.47. The transannular Ti−C bonds are much longer than those in TiC_3. The calculated harmonic vibrational frequency for the symmetric Ti−C stretching vibration being 472 cm^{-1} and has the highest calculated intensity (62 km/mol). Our calculated value is, indeed, in good agreement with the experimental value for Ti−C absorption in TiC_4 (440 cm^{-1}). The atomic charges derived from the Mulliken population analysis for the linear and fan structures are shown in Figure 6. The computed Mulliken population charges suggest the Ti−C bonds to have ionic character, as a consequence of charge transfer from titanium to the carbons. They are associated with appreciable dipole moments owing to the significant charge transfer. The reaction of titanium with carbon clusters giving rise to TiC_n is calculated to be exothermic. Exothermicity depends on the number of Ti−C bonds created as well as the nature of the individual bonds. The linear TiC_n (**I**) isomer has a single Ti−C multiple bond, while structure **VI** has n Ti−C bonds. The carbon−carbon bonds in the fan and linear structures are around 1.3 Å, which corresponds to the carbon−carbon double bond. The energetic gains from several Ti−C bonds are larger than that from a single Ti−C multiple bond in the linear structure. However, in structure **VI**, the carbon chain is no longer linear and the rings are strained. The strain in the ring increases its energy and hence is a destabilizing factor. However, in both TiC_3 and TiC_4 systems, the gain due to several Ti−C bonds overcomes the ring strain energy and hence the fan structures are the most stable.

Nonplanar Structures. Bicyclo[1.1.1] and tricyclo[1.1.1.0] structures, namely, with carbons in the bridgehead positions **XIV** or with a carbon and a titanium in the bridgehead **XV** centers,

have been considered for geometry optimization. Such structures have not been included in the global minimum search for LaC_4 or SiC_4. Isomer **XV** is a minimum on all three surfaces and is more stable in its singlet surface. Though **XV** is higher in energy compared to the global minimum and the linear isomer **IX**, it is comparable in energy with the kite isomer. The C−Ti bond distance in **XVt** equals 1.962 Å, and it signifies the existence of a strong bond and the C−C bond distances are of 1.422 Å. The bridgehead Ti−C bond length is 2.143 Å. On the singlet surface, C_{3v} symmetry has been lifted up.

Bicyclic ring **XIV** is a saddle point on singlet and triplet surfaces and has been characterized as a minimum on the quintet surface. In TiC_4, the global minimum is the fan structure with the linear isomer lying roughly 41 kcal/mol energetically above it. Both the kite and tricyclic isomer **XV** are also minima but are disposed, respectively, 59.3 and 58.8 kcal/mol above the global minimum.

To summarize, our investigations on TiC_x ($x = 2, 3, 4$) clusters, systems containing a higher proportion of carbon to the metal (viz., 1:2 in TiC_2, 1:3 in TiC_3, and 1:4 in TiC_4), reveal that the isomers with multiply bonded carbons are more stable compared to multiply bonded titanium. Thus, in carbon-rich plasma, the titanium atom essentially adheres to the C_n chain. This adumbrates the presence of undissociated C_2 units in met-cars, which are produced only in carbon-rich plasma. However, the proportion of metal to carbon in met-cars is 1:1.5, and in order to derive a better insight about the bonding picture in met-cars, we are pursuing our investigations on Ti_yC_x clusters (y:x = 1:1.5).

Conclusions

The results of our calculations confirm that the ground-state molecular structures of TiC_x ($x = 2-4$) clusters are the ring-type structure or the fan isomers with transannular Ti−C bonds. The kite and linear structures also correspond to a minima, however, with higher energies. Besides these planar ring structures, calculations also suggest nonplanar bicyclic and tricyclic minima for TiC_4. CAS(12,12) investigations on TiC_3 reveal that the bond-stretch isomers are related by a level-crossing mechanism. The isomerization process is symmetry-forbidden. The kite cluster can be viewed as an in-plane complex between Ti and a bond of cyclic C_3. The comparison of the preferred geometries of TiC_x ($x = 2-4$) with the analogous group IVA silicon−carbon clusters (SiC_x) being the following: SiC_2 (cyclic, C_{2v} structure) is similar as TiC_2; SiC_3 is rhomboidal as TiC_3 but with transannular C−C bond instead of a Si−C bond; SiC_4 is linear and contrary to TiC_4, which is cyclic. The Ti−C bonds are strongly ionic, and the main energetical difference between the linear and the ring type structures comes from the delocalization of the transferred charge from Ti to the carbons. The calculated vibrational frequency for the Ti−C absorption in TiC_x clusters is in good agreement with the experimental value.

Acknowledgment. This investigation has been supported by grants from the Flemish Science Foundation (FWO).

References and Notes

(1) Guo, B. C.; Kerns, K. P.; Castleman, A. W., Jr. *Science* **1992**, *255*, 1411. Guo, B. C.; Wei, S.; Purnell, J.; Buzza, S.; Castleman, A. W., Jr. *Science* **1992**, *256*, 511.

(2) Wang, L. S.; Li, S.; Wu, H. *J. Phys. Chem.* **1996**, *100*, 19211. Wang, L. S.; Cheng, H. *Phys. Rev. Lett.* **1997**, *78*, 2983. Li, S.; Wu, H.; Wang, L. S. *J. Am. Chem. Soc.* **1997**, *119*, 7417. Dance, I. *J. Chem. Soc., Chem. Commun.* **1992**, 1779. Reddy, B. N.; Khanna, S. N.; Jene, P. *Science* **1992**, *258*, 1640. Chen, H.; Feyereisen, M.; Long, X. P.; Fitzgerald, G. *Phys. Rev. Lett.* **1993**, *71*, 1732. Hay, P. J. *J. Phys. Chem.* **1993**, *97*, 3081. Lou, L.; Guo, T.; Nordlander, P.; Smalley, R. E. *J. Chem. Phys.* **1993**, *99*, 5301.

(3) Reddy, B. V.; Khanna, S. N. *J. Phys. Chem.* **1994**, *98*, 9446; *Chem. Phys. Lett.* **1993**, *209*, 104.

(4) Wei, S.; Guo, B. C.; Purnell, J.; Buzza, S.; Castleman, A. W., Jr. *J. Phys. Chem.* **1992**, *96*, 4166. Cartier, S. F.; May, B. D.; Castleman, A. W., Jr. *J. Phys. Chem.* **1996**, *100*, 8175.

(5) Pilgrim, J. S.; Brock, L. R.; Duncan, M. A. *J. Phys. Chem.* **1995**, *99*, 544. Brock, L. R.; Duncan, M. A. *J. Phys. Chem.* **1996**, *100*, 5654.

(6) Yeh, C. S.; Byun, Y. G.; Afzaal, S.; Kan, S. Z.; Lee, S. A.; Freiser, B. S.; Hay, P. J. *J. Am. Chem. Soc.* **1995**, *117*, 4042. Byun, Y. G.; Kan, S. z.; Lee, S. A.; Kim, Y. H.; Miletic, M.; Bleil, R. E.; Kais, S.; Freiser, B. S. *J. Phys. Chem.*, **1996**, *100*, 6336.

(7) Lee, S.; Gotts, N. G.; von Helden, G.; Bowers, M. T. *Science* **1995**, *267*, 999.

(8) Wang, X. B.; Ding, C. F.; Wang, L. S. *J. Phys. Chem. A* **1997**, *101*, 7699.

(9) Roszak, S.; Balasubramanian, K. *Chem. Phys. Lett.* **1995**, *246*, 20. Roszak, S.; Balasubramanian, K. *J. Phys. Chem.* **1996**, *100*, 8254.

(10) Gingerich, K. A.; Haque, R.; Pelino, M. *High Temp. Sci.* **1981**, *14*, 137.

(11) Gingerich, K. A.; Haque, R.; Pelino, M. *J. Chem. Soc., Faraday Trans.* **1982**, *78*, 341.

(12) Stearns, C. A.; Kohl, F. J. *J. Chem. Phys.* **1971**, *54*, 5180.

(13) Roszak, S.; Balasubramanian, K. *J. Chem. Phys.* **1997**, *106*, 158.

(14) Bauschlicher, Jr.; Siegbahn, P. E. M. *Chem. Phys. Lett.* **1984**, *104*, 331.

(15) Hack, M. D.; Maclagan, R. G. A. R.; Scuseria, G. E.; Gordon, M. S. *J. Chem. Phys.* **1996**, *104*, 6628.

(16) Sumathi, R.; Hendrickx, M. *Chem. Phys. Lett.*, in press.

(17) Campbell, E. E. B. In *Clusters of Atoms and Molecules*; Haberland, H., Ed.; Springer: Berlin, 1994; pp 331−356.

(18) von Helden, G.; Hsu, M. T.; Kemper, P. R.; Bowers, M. T. *J. Chem. Phys.* **1991**, *95*, 3835.

(19) Raghavachari, K. *J. Chem. Phys.* **1986**, *84*, 5672.

(20) Lammertsma, K.; Pople, J. A.; Schleyer, P. v. R. *J. Am. Chem. Soc.* **1986**, *108*, 7.

(21) Nakajima, A.; Taguwa, T.; Nakao, K.; Gomei, M.; Kishi, R. *J. Chem. Phys.* **1995**, *103*, 2050.

(22) Alberts, I. L.; Grev, R. S.; Schaefer, H. F., III. *J. Chem. Phys.* **1990**, *93*, 5046.

(23) Becke, A. D. *J. Chem. Phys.* **1993**, *98*, 5648.

(24) Lee, C.; Yang, W.; Parr, R. G. *Phys. Rev. B* **1988**, *37*, 785.

(25) Wachters, A. J. H. *J. Chem. Phys.* **1970**, *52*, 1033. Wachters, A. J. H. *IBM Technol. Rep. RJ584* **1969**.

(26) Hay, P. J. *J. Chem. Phys.* **1977**, *66*, 4377.

(27) Bauschlicher, C. W., Jr.; Langhoff, S. R.; Barnes, L. A. *J. Chem. Phys.* **1989**, *91*, 2399.

(28) Stewart, R. F. *J. Chem. Phys.* **1970**, *52*, 431.

(29) Rice, J. E.; Horn, H.; Lengsfiels, B. H.; McLean, A. D.; Carter, J. T.; Replogle, E. S.; Barnes, L. A.; Maluender, S. A.; Lie, G. C.; Gutwski, M.; Rude, W. E.; Sauer, S. P. A.; Lindh, R.; Andersson, K.; Chevalier, T. S.; Widmark, P.-O.; Bouzida, D.; Pacansky, G.; Singh, K.; Gillan, C. J.; Carnevali, P.; Swope, W. C.; Liu, B. *Mulliken Version 2.25b, internal release*; IBM Corporation: Almaden, CA, 1995.

(30) MOLPRO is a package of ab initio computer packages written by H.-J.Werner and P. J. Knowles with contributions from J. Almlöf, R. D. Amos, S. Elbert, W. Meyer, E. A. Reinsch, R. Pitzer, and A. J. Stone.

(31) Moore, C. E. Atomic Energy Levels; National Bureau of Standards (U.S.) Circular 467, 1949.

(32) Sudhakar, P. V.; Lammertsma, K. *J. Phys. Chem.* **1992**, *96*, 4830.

(33) Sumathi, R.; Hendrickx, M. Unpublished Results.